analytical chemistry

pubs.acs.org/ac Article

Designing a CRISPR/Cas12a- and Au-Nanobeacon-Based Diagnostic Biosensor Enabling Direct, Rapid, and Sensitive miRNA Detection

Tong Luo, Jiacheng Li, Yao He, Hui Liu, Zhiwei Deng, Xi Long, Qingqing Wan, Jiacheng Ding, Zan Gong, Yanjing Yang,* and Shian Zhong*

Cite This: *Anal. Chem.* 2022, 94, 6566−6573 Read Online

ACCESS | Metrics & More | Article Recommendations | Supporting Information

ABSTRACT: Direct, rapid, sensitive, and selective detection of nucleic acids in complex biological fluids is crucial for medical early diagnosis. We herein combine the trans-cleavage ability of clustered regularly interspaced short palindromic repeats (CRISPR)/Cas12a with Au-nanobeacon to establish a CRISPR-based biosensor, providing rapid miRNA detection with high speed and attomolar sensitivity. In this strategy, we first report that the trans-cleavage activity of CRISPR/cas12a, which was previously reported to be triggered only by target ssDNA or dsDNA, can be activated by the target miRNA directly. Therefore, this method is direct, i.e., does not need the conversion of miRNA into its complementary DNA (cDNA). Meanwhile, as compared to the traditional ssDNA reporters and molecular beacon (MB) reporters, the Au-nanobeacon reporters exhibit improved reaction kinetics and sensitivity. In this assay, the miRNA-21 could be detected with very high sensitivity in only 5 min. Finally, the proposed strategy enables rapid, sensitive, and selective miRNA determination in complex biological samples, providing a potential tool for medical early diagnosis.

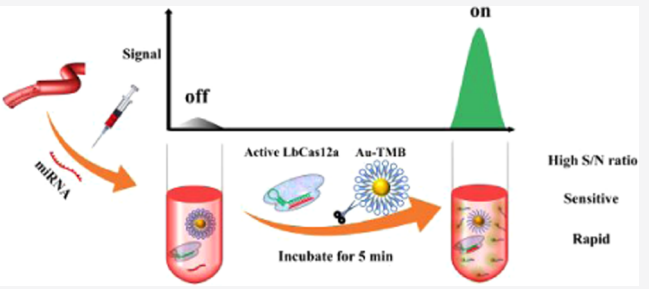

The ability to directly and rapidly detect nucleic acids with high sensitivity and selectivity in complex biological fluids is crucial for medical diagnosis and monitoring.[1−5] Recently, clustered regularly interspaced short palindromic repeats (CRISPRs)-based diagnostics (CRISPR-Dx), such as SHERLOCK,[6] DETECTR,[7] and others,[8−16] have attracted great attention in biochemical analysis and medical diagnoses due to some notable advantages, such as a mild reaction temperature, excellent recognition specificity, and high-efficiency signal amplification capabilities. Within the CRISPR/Cas family, CRISPR/Cas12a has been reported to possess a unique trans-cleavage effect (collateral effect), which could indiscriminately cleave the ambient single-stranded DNA (ssDNA) after binding of a matching target DNA.[7] This crRNA-programmed ssDNase activity has been widely applied to the development of novel biosensing techniques for the detection of nucleic acid, small molecules, proteins, and bacteria. For example, Lu et al. exploited CRISPR/Cas12a and ssDNA fluorescence reporters (which are labeled with a fluorophore and quencher pair at the two ends) to quantitatively detect ATP and Na^+ with high specificity and simplicity.[17] Choi et al. developed a Cas12a-based nucleic acid amplification-free fluorescent biosensor to detect cfDNA by a metal-enhanced fluorescence (MEF).[18] Zhang et al. reported a stable and sensitive Lbcas12a-based diagnostics method for DNA detection using a labeled linear DNA-modified AuNPs as reporters.[19] All these findings prove that the CRISPR/Cas12a system possesses enormous potential in the analysis.

Encouraged by these pioneering studies, we are interested in expanding the application scope of Cas12a to miRNA sensing using nanobeacons as the reporter. Nanobeacon, which combined the advantages of MBs and the excellent properties of nanomaterials, including a highly efficient fluorescence quenching effect, cellular penetration, and different effects on enzyme activity (enhancement, inhibition, or noninfluence), has been applied to design numerous nanoprobes in biology and medicine.[20−26] To date, the properties of nanobeacon have been exploited for a broad spectrum of applications in biosensor construction,[27,28] molecular logic gates,[29−31] and drug delivery.[32−34] Given the success of nanobeacons in biosensing, the coupling of CRISPR/Cas and nanobeacons might provide a new paradigm for the development of CRISPR-based diagnostics. In addition, the loop of MBs on AuNPs may be more possibly accessed by the CRISPR/Cas protein due to the spatial confinement effect[35] and "standing-up" hairpin protrusions,[36] thus resulting in a higher digestive rate and efficiency of MBs as compared to that of linear ssDNA. Hence, we speculated that using nanobeacon as

Received: January 24, 2022
Accepted: April 12, 2022
Published: April 22, 2022

https://doi.org/10.1021/acs.analchem.2c00401
Anal. Chem. 2022, 94, 6566−6573

Scheme 1. Schematic Illustration of the Trans-Cleavage Activity of CRISPR/LbCas12a on AuNPs

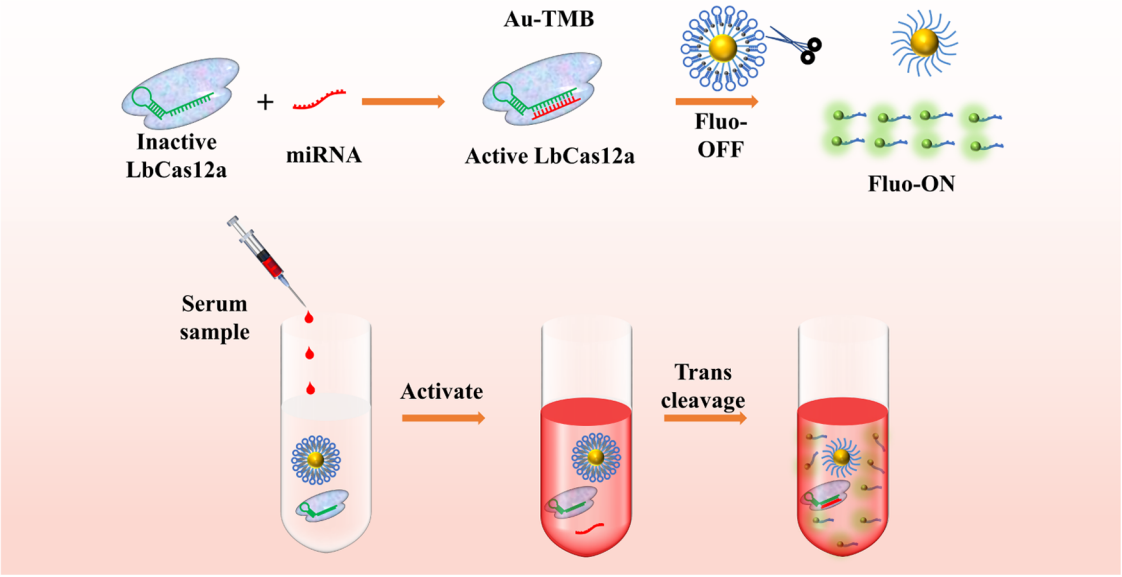

reporters can endow the CRISPR-based diagnostics methods with a high detection sensitivity and fast detection speed.

Aiming at this goal, herein, we for the first time combined CRISPR/Cas12a with AuNP-based nanobeacons to develop a CRISPR-Dx method for the rapid and sensitive detection of miRNA biomarkers. This assay is demonstrated to be direct, rapid, and sensitive. It is noteworthy that the target miRNA could directly activate the collateral cleavage activity of CRISPR/Cas12a, which has previously been reported to be triggered only by target ssDNA or dsDNA. Therefore, this method does not require the conversion of miRNA into cDNA, avoiding contamination of genomic DNA. Moreover, due to the high turnover efficiency of LbCas12a/crRNA-mediated catalysis and the advantages of Au-nanobeacons, as little as 10 fmol of the target miRNA can be detected in only 5 min. Furthermore, the practical application of this strategy in quantifying miRNAs in complex biological samples (serum) was also demonstrated. These results indicate that this CRISPR/Cas12a- and Au-nanobeacon-based method promises great potential for miRNA-related molecular diagnosis and clinical research.

EXPERIMENTAL SECTION

Materials and Reagents. EnGen LbCas12a was purchased from New England Biolabs (Ipswich, MA). All of the DNA samples were purchased from Sangon Biotech (Shanghai China). The sequence and modifications of the DNA are shown in Table S1. DEPC-treated water and PBS solution were also purchased from Sangon Biotech (Shanghai, China). AuNPs were prepared according to a literature method.[37]

Preparation of Au-TMB Reporter. The AuNPs of different sizes were prepared according to the literature.[38,39] Briefly, a 1% HAuCl solution was mixed with 0.25 mM trisodium citrate, then 0.6 mL 0.1 M $NaBH_4$ was added to the mixture quickly under stirring. The solution turned pink immediately, indicating the synthesis of 7 nm AuNPs. Furthermore, 20 mL of aqueous solution of different concentrations of $HAuCl_4$ (AuNPs-13 nm: 1%; AuNPs-25 nm: 1%) was brought to boil to 100 °C. Then, 1.25 mL of trisodium citrate of 38.8 mM or 1 mL of trisodium citrate of 136 mM was added to the above two aqueous solutions, respectively, with vigorous stirring. The color changed from yellow to wine red, indicating the formation of AuNPs. The AuNPs were further refluxed for another 15 min; then, the solutions were cooled to room temperature. Such solutions were centrifuged for 20 min at 5000 rpm and the obtained supernatant was stored at 4 °C for further use.

The FAM-labeled thiolated molecule beacon with a 10-unit T spacer (TMB) was modified to the surface of AuNPs through the freezing method according to the literature.[40] Briefly, the TMB was treated with 5 mM TCEP for 1 h. Next, such TMB (100 μM, 3 μL) was mixed with AuNPs (13 nm, 10 nM, 100 μL). Then, the mixture was put at −20°C in a laboratory freezer for 2h. After thawing at room temperature, the product was centrifuged (21 000g, 30 min, 4 °C) three times to remove the rest of the DNA strands. The prepared Au-TMB was dispersed in ultrapure water and stored at 4 °C.

Trans-Cleavage Ability of LbCas12a on MB. The ability of LbCas12a to digest MB was explored by 15% polyacrylamide gel electrophoresis (PAGE, 80 V,120 min).

Real-Time Fluorescence Monitoring Test. LbCas12a (30 nM) and the corresponding crRNA were incubated in 1× NEB 2.1 buffer at a final ratio of 1:1.25 for 30 min. Then, real-time fluorescence scanning was started immediately after adding Au-TMB and target.

Cleavage Activity of LbCas12a on Au-TMB. LbCas12a (30 nM) and the corresponding crRNA-21 were incubated in 1× NEB 2.1 buffer at a final ratio of 1:1.25 for 30 min. Then, the target and the Au-TMB reporter were added to the Cas12a/crRNA complex and incubated for 5 min. The fluorescence of the final reactant was measured by the FL-2700 fluorescence spectrometer.

Stability Test. The real-time fluorescence signals of three different groups (1 nM Au-TMB with 1× NEB, 1 nM Au-TMB with 1× NEB and 1 nM inactivated LbCas12a-crRNA-21 complex, and 1 nM Au-TMB with 1× NEB and 1 nM activated LbCas12a-crRNA-21 complex) were measured by an FL-2700 fluorescence spectrometer using time scan model to test the

https://doi.org/10.1021/acs.analchem.2c00401
Anal. Chem. 2022, 94, 6566−6573

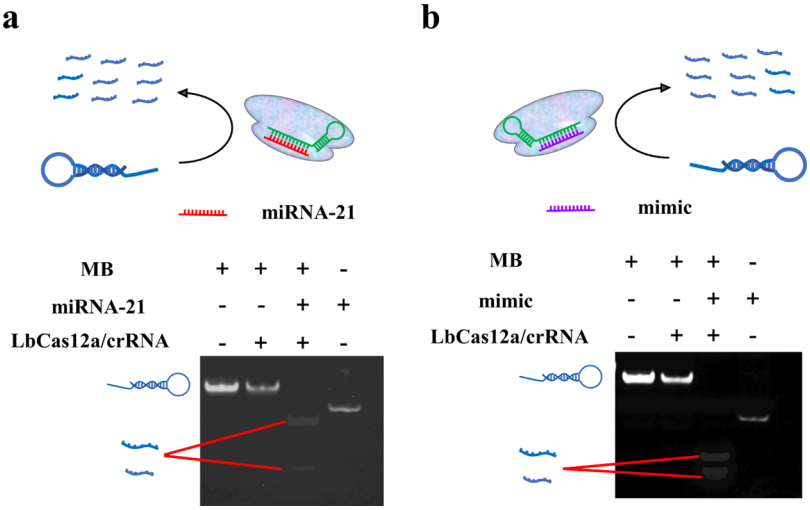

Figure 1. Trans-cleavage ability of LbCas12a/crRNA/Target complex on MB. Activator of (a, b) is miRNA-21 and miRNA-21 analogues (mimic). We found that MB can only be digested in the presence of an activator.

stability of Au-TMB. To test the stability of biosensor in complex environment, we mixed the TMB (200 nM) or Au-TMB (1 nM AuNPs with 200 nM TMB) with 100% fetal bovine serum (100% FBS) or DNase I (1 U/mL). After mixing, its fluorescence signal was immediately measured by an FL-2700 fluorescence spectrometer using the time scan model.

Size Effect of the Gold Nanoparticles on the Recorded Fluorescence Signal. Nine types of Au-TMB with different sizes (7, 13, 25 nm) and different surface densities (high, medium, low) were prepared to test the size effect of gold nanoparticles. Briefly, LbCas12a (20 nM) and the corresponding crRNA were incubated in 1× NEB 2.1 buffer at a final ratio of 1:1.25 for 30 min. Then, the target and Au-TMB reporters with different sizes and densities were added to the Cas12a/crRNA complex and incubated for 5 min. The fluorescence of the final reactant was measured by the FL-2700 fluorescence spectrometer.

Ability to Discriminate Single Mismatched miRNA and Target miRNA. LbCas12a (10 nM) and the corresponding crRNA-21 were incubated in 1× NEB 2.1 buffer at a final ratio of 1:1.25 for 30 min. Then, the mixture of the target (miRNA-21, single mismatched miRNA-21, random sequence) and Au-TMB reporters was added into the Cas12a/crRNA complex, respectively, and incubated for 5 min. The fluorescence of the final reactant was measured by the FL-2700 fluorescence spectrometer.

Detection of Serum Samples Using LbCas12a with the Au-TMB Reporter. The healthy human serum examples were supplied by the Xiangya Hospital Central South University (Changsha, China). The serum sample was centrifuged for 10 min at 4 °C (10 000*g*).[19] Ten microliters of the supernatant mixed with 90 μL of 1× NEB 2.1 buffer was heated at 95 °C for 10 min to inactivate deoxyribonuclease. Finally, different concentrations of miRNA-21 or miRNA-21 analogues were added to the serum sample. The serum sample containing the target was detected using a Cas12a-Au-TMB system. The detecting procedure is the same as that described above.

■ RESULTS AND DISCUSSION

The principle of the designed Cas12a/crRNA- and Au-nanobeacon-based miRNA detection platform is illustrated in Scheme 1. First, the hairpin DNA, which consists of a 5′ thiol and a stem-loop-stem sequence and is terminated at the 3′ end with a fluorophore, was immobilized onto the surface of the 13 nm AuNPs. The fluorescence of the fluorophore is efficiently quenched as a result of the close contact between fluorophores and the AuNP surface. In the absence of the target miRNA, Cas12a stayed inactive and nanobeacon remained in an intact state. Upon addition of target miRNA, the hybridization of crRNA and miRNA could activate the cleavage activity of Cas12a to cleave the hairpin DNA attached to AuNPs. Therefore, the fluorophores are released in the solution, leading to an increased fluorescence signal.

CRISPR/Cas12a has recently been discovered to unleash its indiscriminate single-stranded DNase activity by binding to target ssDNA or dsDNA. In this paper, we surprisingly found that miRNA could also activate the trans-cleavage activity of Lbcas12a. To substantiate that the target miRNA could trigger the trans-cleavage activity of Cas12a-crRNA, we investigated the degradation of MBs substrates in the presence of miRNA using PAGE. MiRNA-21, which is involved in several serious diseases, such as breast cancer,[41] is selected as the model target. As observed in Figure 1a, the MB substrates are digested into random short fragments by Lbcas12a in the presence of crRNA and miRNA-21, confirming that the miRNA activator could activate the ssDNA cleavage activity of LbCas12a-crRNA. When the target is replaced by the corresponding miRNA-21 mimic, the same results are observed (Figure 1b). Meanwhile, MB substrates are degraded rapidly by the activated LbCas12a such that no intact substrate is detected after 5 min (Figure S1). These results demonstrate that target miRNA can trigger the trans-cleavage of LbCas12a as well as ssDNA.

Then, Au-nanobeacon reporters were prepared by modifying AuNPs with the MB strands through the thiolate-Au chemistry. The transmission electron microscopy (TEM) image was first carried out to characterize the size of AuNPs. As shown in Figure S2a, the average size of AuNPs was about 13 nm. In addition, as observed in Figure S2b, the hydrodynamic diameter of AuNP-nanobeacons (about 18 nm) characterized by dynamic light scattering (DLS) was larger than that of AuNPs (about 13 nm), which might be because of the conjugation of the nanobeacons on the AuNP

https://doi.org/10.1021/acs.analchem.2c00401
Anal. Chem. 2022, 94, 6566−6573

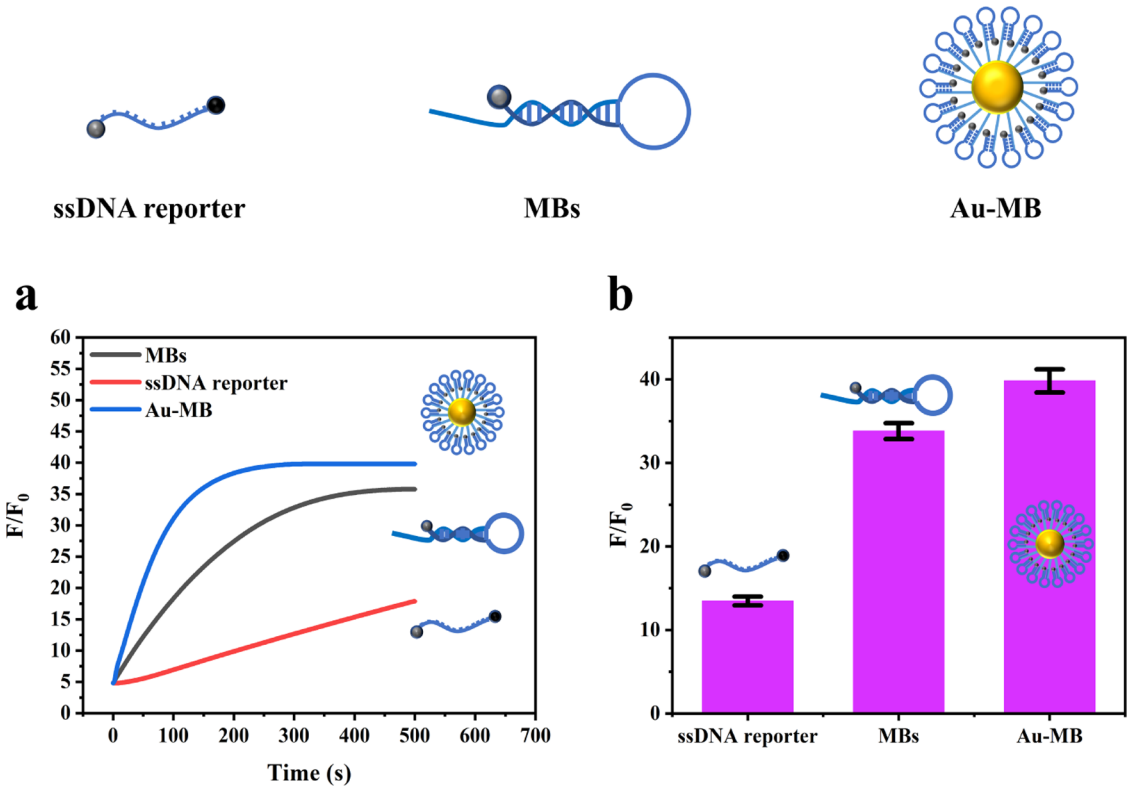

Figure 2. Trans-cleavage effect of the LbCas12a/crRNA complex on different substrates. The LbCas12a/crRNA complex was activated by miRNA-21. The results of (a) real-time comparison and (b) fluorescence response suggest that the Au-MB can be degraded in 5 min and display the highest S/B ratio.

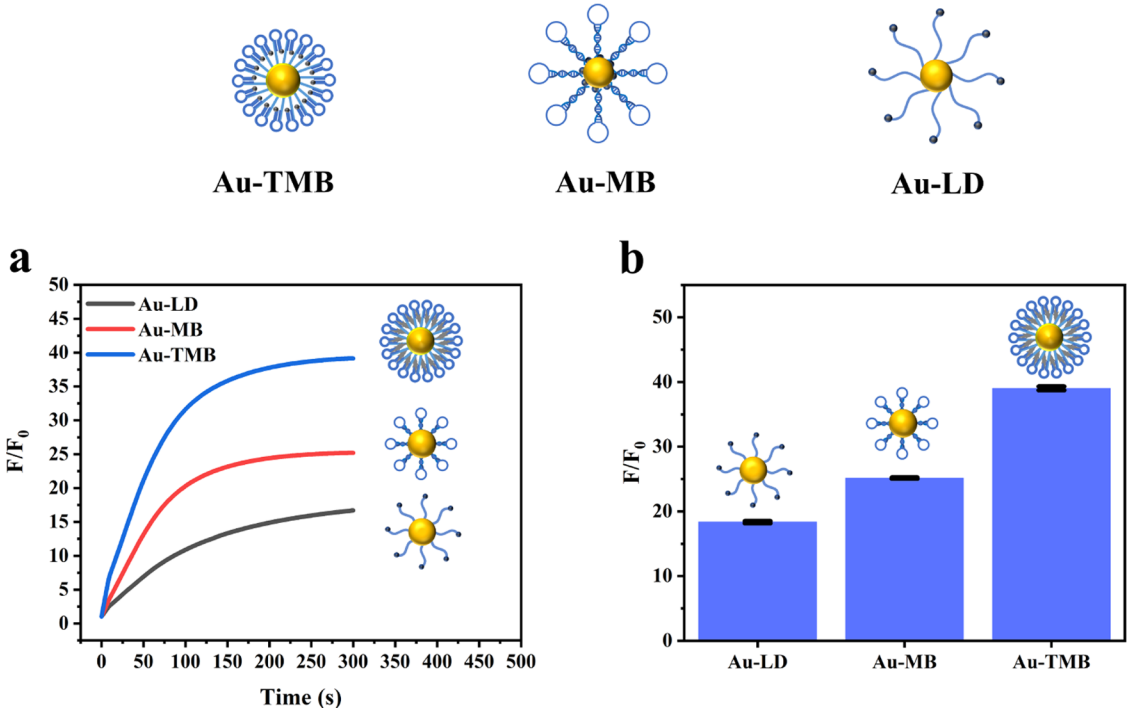

Figure 3. Trans-cleavage activity of LbCas12a/crRNA/Target complex on gold nanoparticles modified with DNA in a different conformation. The activator of (a) real-time comparison and (b) fluorescence response is miRNA-21. The results demonstrate that the degradation rates of different chains are basically the same, but Au-TMB shows a higher S/B ratio.

surface. The ultraviolet−visible (UV−vis) absorption spectra verified this result because the maximum absorption peak of the AuNPs was red-shifted from 518 to 523 nm upon the formation of the Au-nanobeacons (Figure S2c). By incubating the Au-nanobeacons with dithiothreitol (DTT), the obvious fluorescence increase also confirmed the successful modifica-

https://doi.org/10.1021/acs.analchem.2c00401
Anal. Chem. 2022, 94, 6566−6573

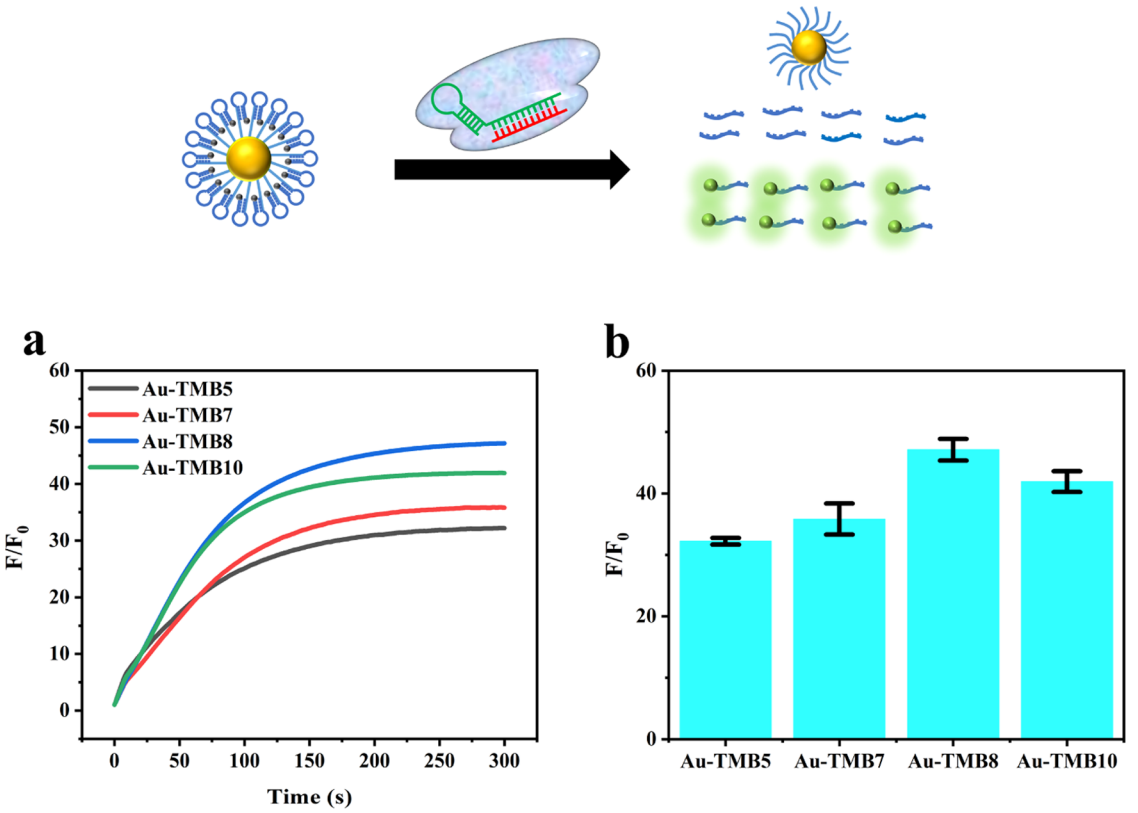

Figure 4. Trans-cleavage activity of LbCas12a/crRNA/Target complex on gold nanoparticles modified with DNA hairpin of various base pairs. The activator of (a) real-time comparison and (b) fluorescence response is miRNA-21. With the increase in base pairs in the stem, the S/B ratio is gradually enhanced, and eight base pairs reach the maximum.

tion and quenching of the fluorescent hairpin DNA strands on the AuNPs (Figure S2d). These results indicated that the Au-nanobeacon reporter was successfully prepared.

Next, we compared the enzyme activity of CRISPR/Cas12a to those of an Au-nanobeacon reporter, MB reporter, and ssDNA reporter, which were widely used reporters in biosensors, after recognizing the targeted miRNA. Real-time monitoring of fluorescence response (F/F_0) was performed to investigate the collateral DNase activity of CRISPR/Cas12a on Au-nanobeacon reporter, MBs reporter, and ssDNA reporter, respectively. As can be observed in Figure 2a, the Au-nanobeacon reporter reached a saturated fluorescence signal in only 4 min, while the MBs reporter and ssDNA reporters required approximately 8 min and 1 h (Figure S3) to reach the maximum fluorescence signal, indicating an obvious improvement of the trans-cleavage kinetics in the Au-nanobeacon reporter. In addition, the maximum fluorescence response signal (F/F_0) of Au-nanobeacon reporter and MBs reporter were compared. As shown in Figure 2b, there was a much higher fluorescence response for Au-nanobeacon reporter as compared to MBs reporter and ssDNA reporter. These results demonstrated that Lbcas12a exhibited an unusually high activity toward Au-nanobeacon reporters as compared to free MBs and ssDNA, which suggested the high processivity of Lbcas12a for the Au-nanobeacon reporter. This occurred because the local concentration of substrates in the Au-nanobeacon reporter was increased by virtue of the spatial confinement effect. These consistent results proved that the LbCas12a/crRNA and Au-nanobeacon platform could be used for miRNA detection with high speed and good sensitivity.

Several research studies have reported that the performance of DNA-modified AuNP-based biosensors is highly dependent on the conformation of surface DNA. Therefore, we investigated the conformation effect of the surface DNA of AuNPs on the trans-cleavage activity of CRISPR/Cas12a. Three kinds of DNA-AuNPs were prepared. Two of them (Au-MB and Au-TMB) were constructed with the MBs either bound directly to the nanoparticle surface or bound through a 10-unit T spacer. The AuNPs of another group (Au-LD) were functionalized with linear DNA strands. As observed in Figure 3, the degradation rate and fluorescence response signals of Au-LD were lower than that of Au-TMB and Au-MB. Meanwhile, a higher fluorescence response signal was observed in the group of Au-TMB as compared to that of Au-MB. These results demonstrated that hairpin DNA on AuNPs was more likely degraded as compared to linear DNA, and the employment of T spacer significantly increased the degradation rate of nanobeacon. The reason may be that the "standing-up" orientation and tense loop of MBs are more beneficial for digestion by Lbcas12a than the "lying-down" conformation of linear DNAs on the AuNP surface. Thus, the design of Au-TMB was applied in the following experiments.

Considering that the number of base pairs in the stem might influence the performance of this nanobeacon biosensor due to the steric hindrance and different Tm, we prepared a series of MBs with different longer base-pair stems to examine the collateral DNase activity of LbCas12a on nanobeacon. With a longer stem from H-1 to H-4, the Tm shifted to a higher point (Figure S4). Through the real-time fluorescence monitoring experiments, we found that the change in stem lengths did not affect their response time, all of the fluorescence enhancements

https://doi.org/10.1021/acs.analchem.2c00401
Anal. Chem. 2022, 94, 6566−6573

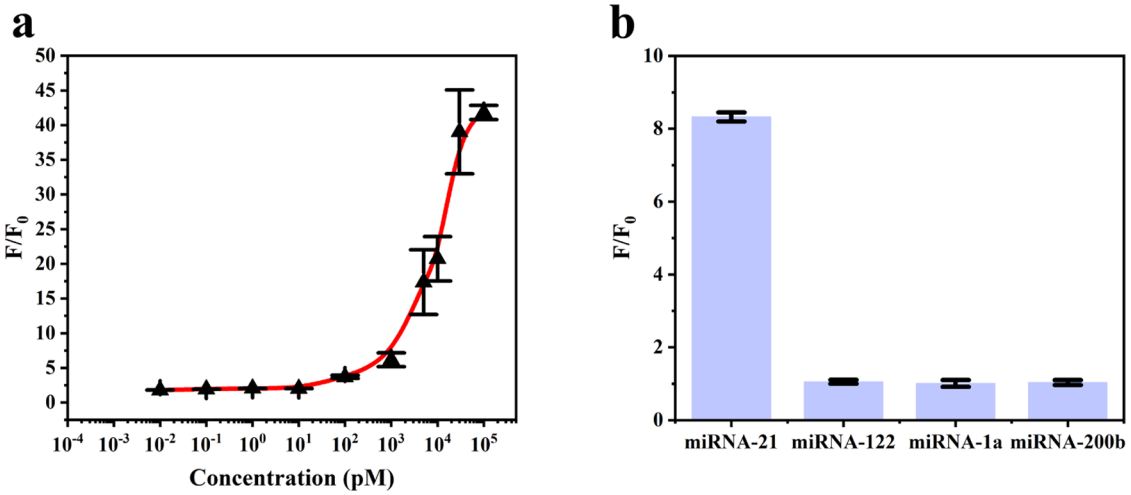

Figure 5. (a) Limit detection of CRISPR/LbCas12a Au-nanobeacon-based sensor on miRNA-21. (b) Detection specificity of the CRISPR/Cas12a and nanobeacon-based sensor. The detection limit of the CRISPR/LbCas12a Au-TMB system is 10 fM and the detection system has good specificity.

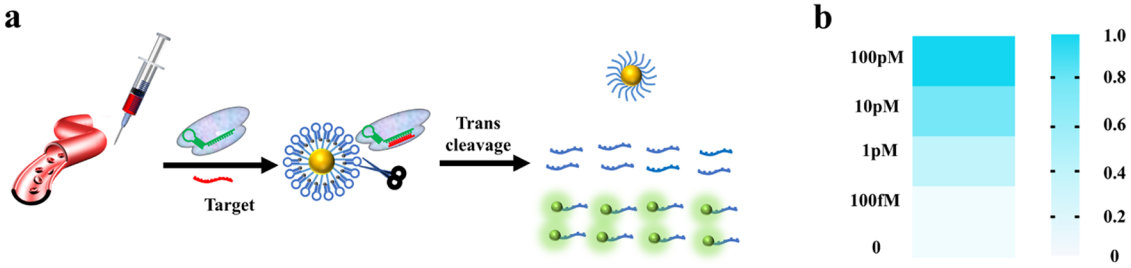

c

Sample	Add(pM)	Found (pM)	Recovery(%)	RSD(%) (n=3)
miRNA-21	100	71	71	4.33
	10	9.6	96	8.89
	1	0.68	68	6.84
	0.1	0.086	86	2.24

Figure 6. Application of CRISPR/LbCas12a Au-nanobeacon-based sensor in serum sample analysis. (a) Schematic of miRNA-21 detection in serum samples. (b) Heat map analysis of different concentrations of miRNA-21. (c) Recovery experiment for the detection of different concentrations of miRNA-21 in serum samples.

were completed in about 4 min (Figure 4a). However, the maximum fluorescence response signals of these nanobeacons were different. The Au-nanobeacon biosensor with eight base pairs in the stem of surface MBs exhibited the highest fluorescence response signals (Figure 4b). If the base pair's length is too short or too long, the fluorescence response signals decreased. A too-short stem might result in a high signal background, which might decrease the S/B ratio. As for the lower fluorescence response signals in a longer stem in MBs, it might happen because LbCas12a/crRNA spent more time degrading than the longer MBs. These results demonstrated that the number of base pairs in the stem influenced the performance of the nanobeacon biosensors, although Cas12a could indiscriminately cleave the ssDNA/dsDNA hybrid complex. Therefore, the nanobeacon biosensor based on eight base pairs in the stem of MBs was employed in the following experiments.

To achieve the optimal performance of nanobeacon biosensors for miRNA-21 detection, other key experimental parameters, including the density of MB strands, AuNPs size, and the concentration of nanobeacons, were optimized (Figure S5). The S/B ratio varied greatly from 18 to 28 when the DNA density was tuned from low to high. We suspected that the high S/B ratio for densely packed nanobeacon possibly originated from the greater accessibility of the Lbcas12a to "standing-up" strands in nanobeacon, resulting in the higher cleavage efficiency and release of more fluorescent molecules. The effect of AuNPs size on the trans activity of this biosensor was also studied. AuNPs measuring 7 nm, 13 nm, and 25 nm were selected, and their TEM images are shown in Figure S6. The fluorescence data (Figures S7 and S8) demonstrated that the nanobeacon using 13 nm AuNPs with high MB density gave the best S/B ratio. In addition, as shown in Figure S9, nanobeacon biosensors achieved the best cleavage activity at the concentration of 1 nM.

To further depict the detection range of this approach, a series of samples containing different concentrations of target miRNA have been tested using the optimized conditions. The

https://doi.org/10.1021/acs.analchem.2c00401
Anal. Chem. 2022, 94, 6566−6573

fluorescence of the nanobeacon biosensors, after the addition of target miRNA with concentrations ranging from 10 fM to 100 nM, is plotted in Figure 5a. In this nanobeacon-based assay, it can be observed that there is a gradual increase in the fluorescence intensity with an increase in the concentration of target miRNA from 10 pM to 10 nM. A detection limit of 10 fM was achieved according to the 3σ standard rule (Figure S10). Based on the same calculation method, the detection limit of this sensor toward miRNA-21 mimic was as low as 10 aM (Figure S11). Thus, this sensor exhibited high sensitivity in detecting nucleic acid. Moreover, a comparison between this biosensor and previously reported studies was carried out. As shown in Table S2 (Supporting Information), the sensitivity of our sensor was comparable to or better than that of previous works. In addition, the detection specificity of the CRISPR/Cas12a and nanobeacon-based sensor for miRNA-21 relative to single-base mismatch target and other interfering miRNAs was studied. Figures S12 and 5b show that the fluorescence signals were relatively low in the presence of a single-base-mismatched target and other interfering miRNAs, including miRNA-122, miRNA-1a, and miRNA-200b. By contrast, the fluorescence signal was significantly enhanced in the presence of miRNA-21, manifesting the specific response of this Cas12a- and Au-nanobeacon-based sensor for miRNA-21. The stability of this sensor in solution was also tested by monitoring the real-time fluorescence signal. As shown in Figure S13, the CRISPR/LbCas12a Au-nanobeacon-based sensor exhibited good signal stability with or without miRNA-21.

To evaluate the practicability and potential of clinical application of this CRISPR/Cas12a and nanobeacon-based sensor, we studied its stability in a complex system. The MBs were also tested as a comparison. As expected, the nanobeacon reporters treated with Dnase I (Figure S14a) or 100% FBS (Figure S14b) were not obviously digested. However, the MBs were degraded rapidly by Dnase I and 100% FBS. These results demonstrated that the nanobeacon reporter possessed higher biological stability as compared to MBs and could be used for miRNA detection in real samples. In addition, the performance of this CRISPR/Cas12a and nanobeacon-based sensor in the detection of miRNA-21 in the human serum sample was also investigated (Figure 6a). The 10% diluted human serums spiked with different concentrations of miRNA-21 were detected by the CRISPR/Cas12a and nanobeacon-based sensors. In Figure 6b, the detection signal of the LbCas12a/Au-nanobeacon biosensor increased as the concentration of miRNA-21 increased, demonstrating that LbCas12a/Au-nanobeacon can detect the target in the real sample. Figure 6c shows that the miRNA recovery ranged from 68 to 96%, and the relative standard deviation ranged from 2.2 to 8.9%, demonstrating the reliability of the approach for low-abundance miRNA detection in a diluted human serum sample. These results verified the applicability of this CRISPR/Cas12a and nanobeacon-based miRNA-triggered method in clinical diagnosis.

CONCLUSIONS

In summary, we developed a novel biosensor for direct, rapid, and sensitive detection of miRNA by integrating a CRISPR/Cas12a system and nanobeacon. As a result, multiple advantages were demonstrated. First, we demonstrated for the first time that LbCas12a bound to target miRNA can unleash its trans-cleavage activity either. Thus, this assay was straightforward, did not require converting the target miRNA into a cDNA, and was technically easy to achieve. Second, due to the spatial confinement effect, the reaction kinetics for target miRNA binding Cas12a-catalyzed signal generation was significantly improved by comparison with ssDNA reporter and MBs. In addition, the nanobeacon-based CRISPR/Cas12a biosensor also exhibited good sensitivity, selectivity, and stability. The LOD for the miRNA-21 detection was as low as 10 fM, and this method was successfully applied for miRNA-21 in complex biological samples. We anticipate that this new strategy to be further explored for more in biological and biomedical studies.

ASSOCIATED CONTENT

Supporting Information

The Supporting Information is available free of charge at https://pubs.acs.org/doi/10.1021/acs.analchem.2c00401.

Electrophoresis results of MBs, characterization of Au-TMB, fluorescence result of ssDNA reporter, secondary structures of H-1, H-2, H-3, and H-4, fluorescence results of Au-TMB surface density, fluorescence results of Au-TMB reaction concentration, stability test of Au-TMB, limit of detection on miRNA-21 and mimic, TEM of AuNPs of different sizes, fluorescence signal of AuNPs of different sizes with different density of TMB, S/N ratio of AuNPs of different sizes with different density of TMB, discrimination ability of CRISPR/LbCas12a Au-TMB system on a single-base mismatch, stability tests, sequences of oligonucleotides used in this work, and summary of other miRNA biosensors (PDF)

AUTHOR INFORMATION

Corresponding Authors

Yanjing Yang − *College of Chemistry and Chemical Engineering, Central South University, Changsha 410083, P. R. China*; Email: yangyanjing@csu.edu.cn

Shian Zhong − *College of Chemistry and Chemical Engineering, Central South University, Changsha 410083, P. R. China*; orcid.org/0000-0002-0729-2304; Email: zhongshian@aliyun.com

Authors

Tong Luo − *College of Chemistry and Chemical Engineering, Central South University, Changsha 410083, P. R. China*

Jiacheng Li − *College of Chemistry and Chemical Engineering, Central South University, Changsha 410083, P. R. China*

Yao He − *College of Chemistry and Chemical Engineering, Central South University, Changsha 410083, P. R. China*

Hui Liu − *College of Chemistry and Chemical Engineering, Central South University, Changsha 410083, P. R. China*

Zhiwei Deng − *College of Chemistry and Chemical Engineering, Central South University, Changsha 410083, P. R. China*

Xi Long − *College of Chemistry and Chemical Engineering, Central South University, Changsha 410083, P. R. China*

Qingqing Wan − *College of Chemistry and Chemical Engineering, Central South University, Changsha 410083, P. R. China*

Jiacheng Ding − *College of Chemistry and Chemical Engineering, Central South University, Changsha 410083, P. R. China*

Zan Gong − *College of Chemistry and Chemical Engineering, Central South University, Changsha 410083, P. R. China*

https://doi.org/10.1021/acs.analchem.2c00401
Anal. Chem. 2022, 94, 6566−6573

Complete contact information is available at:
https://pubs.acs.org/10.1021/acs.analchem.2c00401

Author Contributions

All authors have given approval to the final version of the manuscript.

Notes

The authors declare no competing financial interest.

■ ACKNOWLEDGMENTS

This work was supported by the National Natural Science Foundation of China (21576295 and 21804143) and the Natural Science Foundation of Hunan Province (2020JJ4686).

■ REFERENCES

(1) Zhou, H.; Liu, J.; Xu, J. J.; Zhang, S. S.; Chen, H. Y. *Chem. Soc. Rev.* **2018**, *47*, 1996−2019.
(2) Shin, S.; Jung, Y.; Uhm, H.; Song, M.; Son, S.; Goo, J.; Jeong, C.; Song, J. J.; Kim, V. N.; Hohng, S. *Nat. Commun.* **2020**, *11*, No. 6033.
(3) Li, M.; Yin, F. F.; Song, L.; Mao, X. H.; Li, F.; Fan, C. H.; Zuo, X. L.; Xia, Q. *Chem. Rev.* **2021**, *121*, 10469−10558.
(4) Lan, L.; Huang, J.; Liu, M. T.; Yin, Y.; Wei, C.; Cai, Q. Y.; Meng, X. X. *Chem. Sci.* **2021**, *12*, 4509−4518.
(5) Kong, J. E.; Wei, Q. S.; Tseng, D.; Zhang, J. Z.; Pan, E.; Lewinski, M.; Garner, O. B.; Ozcan, A.; Di Carlo, D. *ACS Nano* **2017**, *11*, 2934−2943.
(6) Gootenberg, J. S.; Abudayyeh, O. O.; Lee, J. W.; Essletzbichler, P.; Dy, A. J.; Joung, J.; Verdine, V.; Donghia, N.; Daringer, N. M.; Freije, C. A.; Myhrvold, C.; Bhattacharyya, R. P.; Livny, J.; Regev, A.; Koonin, E. V.; Hung, D. T.; Sabeti, P. C.; Collins, J. J.; Zhang, F. *Science* **2017**, *356*, 438−442.
(7) Chen, J. S.; Ma, E.; Harrington, L. B.; Da Costa, M.; Tian, X.; Palefsky, J. M.; Doudna, J. A. *Science* **2021**, *371*, 436−439.
(8) Liang, M. D.; Li, Z. L.; Wang, W. S.; Liu, J. K.; Liu, L. S.; Zhu, G. L.; Karthik, L.; Wang, M.; Wang, K. F.; Wang, Z.; Yu, J.; Shuai, Y. T.; Yu, J. M.; Zhang, L.; Yang, Z. H.; Li, C.; Zhang, Q.; Shi, T.; Zhou, L. M.; Xie, F.; Dai, H. Q.; Liu, X. T.; Zhang, J. Y.; Liu, G.; Zhuo, Y.; Zhang, B. C.; Liu, C. L.; Li, S. S.; Xia, X. K.; Tong, Y. J.; Liu, Y. W.; Alterovitz, G.; Tan, G. Y.; Zhang, L. X. *Nat. Commun.* **2019**, *10*, No. 3672.
(9) Dronina, J.; Bubniene, U. S.; Ramanavicius, A. *J. Nanobiotechnol.* **2021**, *19*, No. 348.
(10) Gong, S. H.; Zhang, S. Q.; Lu, F.; Pan, W.; Li, N.; Tang, B. *Anal. Chem.* **2021**, *93*, 11899−11909.
(11) Feng, W.; Peng, H. Y.; Xu, J. Y.; Liu, Y. M.; Pabbaraju, K.; Tipples, G.; Joyce, M. A.; Saffran, H. A.; Tyrrell, D. L.; Babiuk, S.; Zhang, H. Q.; Le, X. C. *Anal. Chem.* **2021**, *93*, 12808−12816.
(12) Yue, H. H.; Huang, M. Q.; Tian, T.; Xiong, E. H.; Zhou, X. M. *ACS Nano* **2021**, *15*, 7848−7859.
(13) Chen, Y.; Mei, Y. X.; Jiang, X. Y. *Chem. Sci.* **2021**, *12*, 4455−4462.
(14) Dronina, J.; Bubniene, U. S.; Ramanavicius, A. *Biosens. Bioelectron.* **2021**, *175*, No. 112867.
(15) Gong, S. H.; Li, J. J.; Pan, W.; Li, N.; Tang, B. *Anal. Chem.* **2021**, *93*, 10719−10726.
(16) Dronina, J.; Bubniene, U. S.; Ramanavicius, A. *J. Nanobiotechnol.* **2022**, *20*, No. 41.
(17) Xiong, Y.; Zhang, J. J.; Yang, Z. L.; Mou, Q. B.; Ma, Y.; Xiong, Y. H.; Lu, Y. *J. Am. Chem. Soc.* **2020**, *142*, 207−213.
(18) Choi, J. H.; Lim, J.; Shin, M.; Paek, S. H.; Choi, J. W. *Nano Lett.* **2021**, *21*, 693−699.
(19) Fu, X. Y.; Shi, Y. Y.; Peng, F. Q.; Zhou, M.; Yin, Y.; Tan, Y.; Chen, M.; Yin, X.; Ke, G. L.; Zhang, X. B. *Anal. Chem.* **2021**, *93*, 4967−4974.
(20) Jayagopal, A.; Halfpenny, K. C.; Perez, J. W.; Wright, D. W. *J. Am. Chem. Soc.* **2010**, *132*, 9789−9796.
(21) Ma, Y. X.; Mao, G. B.; Huang, W. R.; Wu, G. Q.; Yin, W.; Ji, X. H.; Deng, Z. S.; Cai, Z. M.; Zhang, X. E.; He, Z. K.; Cui, Z. Q. *J. Am. Chem. Soc.* **2019**, *141*, 13454−13458.
(22) Song, S. P.; Liang, Z. Q.; Zhang, J.; Wang, L. H.; Li, G. X.; Fan, C. H. *Angew. Chem., Int. Ed.* **2009**, *48*, 8670−8674.
(23) Wang, J. L.; Huang, J.; Quan, K.; Li, J.; Wu, Y. A.; Wei, Q. M.; Yang, X. H.; Wang, K. M. *Chem. Commun.* **2018**, *54*, 10336−10339.
(24) Xue, C.; Wang, L.; Huang, H.; Wang, R.; Yuan, P.; Wu, Z. S. *ACS Sens.* **2021**, *6*, 4029−4037.
(25) Dong, Z. Z.; Yan, S.; Liu, B.; Hao, Y. C.; Lin, L.; Chang, T. R.; Sun, H.; Wang, Y. S.; Li, H.; Wu, H.; Hang, X. X.; He, S. Q.; Hu, J. M.; Xue, X. Y.; Wu, N.; Chang, L. Q. *Nano Lett.* **2021**, *21*, 4878−4886.
(26) Liu, B.; Zhou, P.; Wang, K. Y.; Gong, S. H.; Luan, M. M.; Li, N.; Tang, B. *ACS Sens.* **2021**, *6*, 1949−1955.
(27) Mascini, M.; Gaggiotti, S.; Della Pelle, F.; Wang, J.; Pingarron, J. M.; Compagnone, D. *Biosens. Bioelectron.* **2019**, *123*, 124−130.
(28) Chen, L. Z.; Chao, J.; Qu, X. M.; Zhang, H. B.; Zhu, D.; Su, S.; Aldalbahi, A.; Wang, L. H.; Pei, H. *ACS Appl. Mater. Interfaces* **2017**, *9*, 8014−8020.
(29) Lv, M. M.; Zhou, W. J.; Fan, D. Q.; Guo, Y. C.; Zhu, X. Q.; Ren, J. T.; Wang, E. R. *Adv. Mater.* **2020**, *32*, No. 1908480.
(30) Zhang, L. L.; Bluhm, A. M.; Chen, K. J.; Larkey, N. E.; Burrows, S. M. *Nanoscale* **2017**, *9*, 1709−1720.
(31) Chatterjee, G.; Dalchau, N.; Muscat, R. A.; Phillips, A.; Seelig, G. *Nat. Nanotechnol.* **2017**, *12*, 920−927.
(32) Ding, Q. W.; Zhan, Q. Q.; Zhou, X. M.; Zhang, T.; Xing, D. *Small* **2016**, *12*, 5944−5953.
(33) Wang, Y.; Xia, K.; Wang, L. C.; Wu, M. X.; Sang, X. J.; Wan, K. M.; Zhang, X. D.; Liu, X. M.; Wei, G. *Small* **2021**, *17*, No. 2005578.
(34) Han, S. Y.; Samanta, A.; Xie, X. J.; Huang, L.; Peng, J. J.; Park, S. J.; Teh, D. B. L.; Choi, Y.; Chang, Y. T.; All, A. H.; Yang, Y. M.; Xing, B. G.; Liu, X. G. *Adv. Mater.* **2017**, *29*, No. 1700244.
(35) Qing, Z. H.; Hu, J. L.; Xu, J. Y.; Zou, Z.; Lei, Y. L.; Qing, T. P.; Yang, R. H. *Chem. Sci.* **2020**, *11*, 1985−1990.
(36) Xue, C.; Zhang, S. B.; Yu, X.; Hu, S. Y.; Lu, Y.; Wu, Z. S. *Angew. Chem., Int. Ed.* **2020**, *59*, 17540−17547.
(37) Fu, X.; Shi, Y.; Peng, F.; Zhou, M.; Yin, Y.; Tan, Y.; Chen, M.; Yin, X.; Ke, G.; Zhang, X. B. *Anal. Chem.* **2021**, *93*, 4967−4974.
(38) Jana, N. R.; Gearheart, L.; Murphy, C. J. *Langmuir* **2001**, *17*, 6782−6786.
(39) Paul, I. E.; Rajeshwari, A.; Satija, J.; Raichur, A. M.; Chandrasekaran, N.; Mukherjee, A. *J. Fluoresc.* **2016**, *26*, 2225−2235.
(40) Liu, B.; Liu, J. *J. Am. Chem. Soc.* **2017**, *139*, 9471−9474.
(41) Yan, H.; Bhattarai, U.; Guo, Z. F.; Liang, F. S. *J. Am. Chem. Soc.* **2017**, *139*, 4987−4990.